Vol. 81 No. 4 pp. 622–636 ACTA GEOLOGICA SINICA Aug. 2007

REE Geochemistry of Fluorite from the Maoniuping REE Deposit, Sichuan Province, China: Implications for the Source of Ore-forming Fluids

HUANG Zhilong[1,*], XU Cheng[1], Andrew McCAIG[2], LIU Congqiang[1], WU Jing[3], XU Deru[4], LI Wenbo[1], GUAN Tao[1] and XIAO Huayun[1]

1 *The Key Laboratory of Ore Deposit Geochemistry, Institute of Geochemistry, Chinese Academy of Sciences, Guiyang, Guizhou 550002, China*

2 *The School of Earth Sciences, University of Leeds, Leeds LS2 9JT, UK*

3 *Department of Geology, Kunming University of Technology and Science, Kunming, Yunnan 650093, China*

4 *Guangzhou Institute of Geochemistry, Chinese Academy of Sciences, Guangzhou, Guangdong 550002, China*

Abstract: Fluorite is one of the main gangue minerals in the Maoniuping REE deposit, Sichuan Province, China. Fluorite with different colors occurs not only within various orebodies, but also in wallrocks of the orefield. Based on REE geochemistry, fluorite in the orefield can be classified as the LREE-rich, LREE-flat and LREE-depleted types. The three types of fluorite formed at different stages from the same hydrothermal fluid source, with the LREE-rich fluorite forming at the relatively early stage, the LREE-flat fluorite in the middle, and the LREE-depleted fluorite at the latest stage. Various lines of evidence demonstrate that the variation of the REE contents of fluorite shows no relation to the color. The mineralization of the Maoniuping REE deposit is associated spatially and temporally with carbonatite-syenite magmatism and the ore-forming fluids are mainly derived from carbonatite and syenite melts.

Key words: fluorite, REE geochemistry, ore-forming fluid, Maoniuping REE deposit

1 Introduction

Rare earth element (REE) geochemistry of fluorite has found a wide application in constraining the source and evolution of ore-forming fluids (Dill et al., 1986; Ekambaram et al., 1986; Constantopoulos, 1988; Eppinger and Closs, 1990; Bau and Dulski, 1995; Cunningham et al., 1998; Fanlo et al., 1998; Coniglio et al., 2000; Monecke et al., 2000; Bühn et al., 2002, 2003; Bau et al., 2003; Alvin et al., 2004; Schwinn and Markl, 2005). The Maoniuping REE deposit, Sichuan Province, China is a large-scale primary light REE deposit. In the primary REE deposits in China, this REE deposit is only smaller in scale than the Bayan Obo REE deposit, Inner Mongolia. Although many scholars have studied this deposit with focus on regional geology (Zhang et al., 1988; Yuan et al., 1995; Wang et al., 2001), ore geology (Yuan et al., 1995; Yang et al., 2000), ore-controlling structures (Jiang, 1992; Wang et al., 2001), ore-forming ages (Yuan et al., 1993; Yuan et al., 1995), fluid inclusion geochemistry (Niu et al., 1997; Xu et al., 2001; Yang et al., 2001; Tian et al., 2006), host magmatic rocks (Xu et al., 2003, 2004) and metallogeny (Pu, 1993; Niu and Lin, 1994; Yuan et al., 1995), the source of the ore-forming fluids is still under debate. Fluorite is the most important gangue mineral in the Maoniuping REE deposit. Yuan et al. (1995) found that the chondrite-normalized REE patterns of fluorite in the deposit are different from those of the REE minerals and other gangue-minerals, but no explanation has been presented for this phenomenon. Based on fluid-melt inclusions in fluorite and the difference in REE geochemistry between the fluorite in the deposit and other hydrothermal fluorite, Niu et al. (1996) suggested that the fluorite in the orefield is of magmatic origin. However, he did not use the REE geochemistry of the fluorite in the deposit to discuss the source of the ore-forming fluids.

We here present new REE data of fluorite in the Maoniuping REE deposit, and discuss mainly the source of the ore-forming fluids based on these data in combination with Sr-Nd-Pb isotopic compositions of fluorite and REE, Sr-Nd-Pb and C-O-H isotopic compositions of rocks and

* Corresponding author. E-mail: huangzhilong@vip.gyig.ac.cn

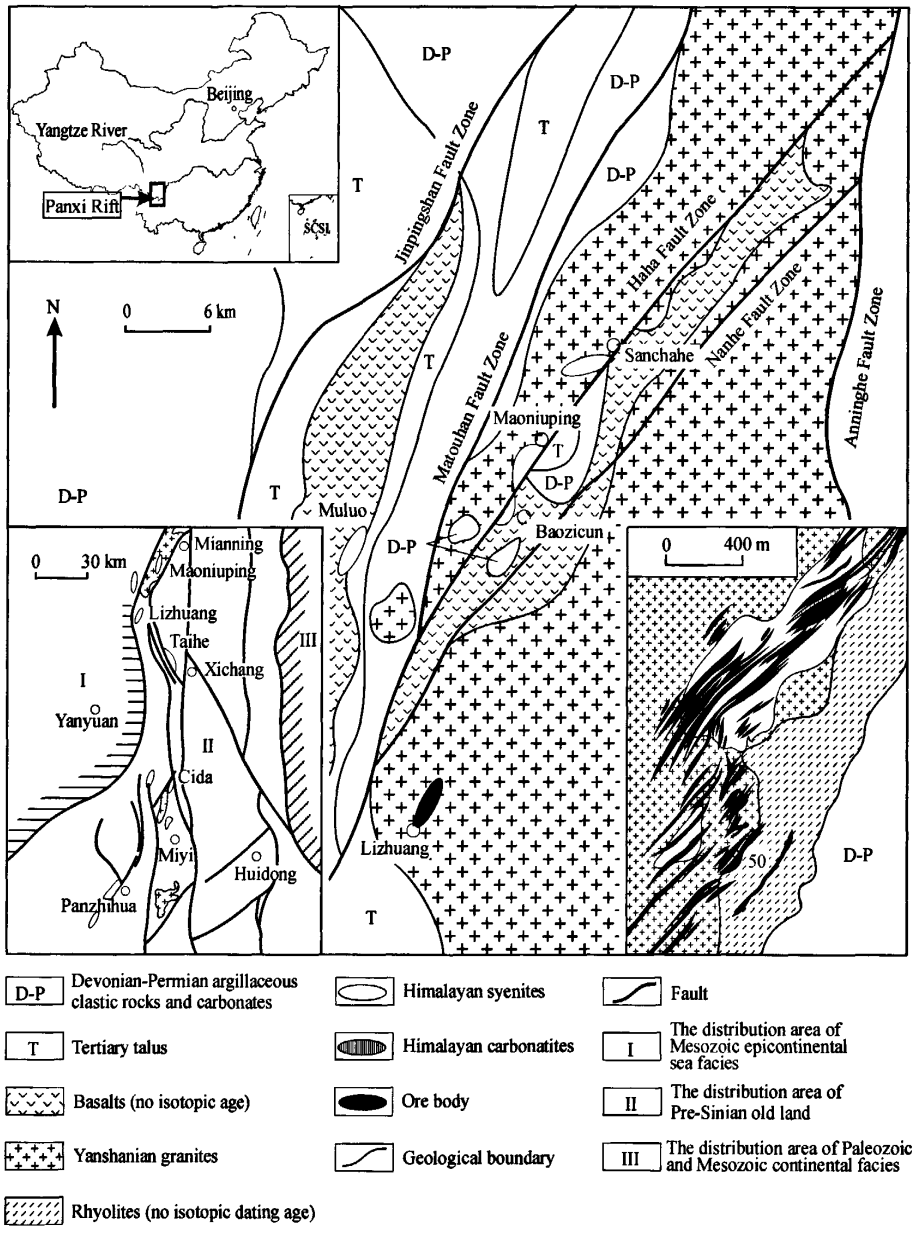

Fig. 1. The geological map of the Maoniuping REE deposit.

other minerals in the orefield.

2 Geology and Basic Geological Features of Fluorite

The Maoniuping REE deposit is one of the largest primary light REE deposits in China, and its REE resources are second to those of the Bayan Obo Fe-Nb-REE deposit. Its REE_2O_3 resources are estimated at over 1.5 million tons, REE_2O_3 grades of various primary ores and the secondary ores (weathered and oxidized) vary from 2.7% to 3.9% and 10.0% to 13.6% respectively (No.109 Geological Team, unpubl report). This deposit is located in the northern part of the Panxi Rift (Fig. 1). In the area of the deposit, the outcrop strata are Devonian-Permian argillaceou clastic carbonate rock and Tertiary talus. The main structures are northeast-trending fault zones including the Jinpingshan, Matoushan, Haha and Nanhe fault zones. Magmatic rocks include the Yanshanian granite (whole-rock U-Pb age of 78 to 134

Ma; Yuan et al., 1993), Himalayan syenite and carbonatite (K-Ar ages of 28 to 48 Ma and 31.7±0.7 Ma, respectively; Yuan et al., 1995), and minor basalt and rhyolite without isotopic age. The Himalayan syenite and carbonatite are spatially and temporally associated with the REE mineralization (Fig. 1). The ore types are mainly barite-bearing pegmatite and calcite-bearing pegmatite with subordinate thin-network aplite. The major ore mineral is bastnaesite and the gangue minerals are mainly fluorite, barite, calcite, feldspar, quartz, mica and aegirine-augite.

Fluorite is one of the major gangue minerals in the Maoniuping REE deposit, and occurs in all types of ores. In the barite-bearing pegmatite ores, fluorite occurs mainly as discontinuous bands and subordinately as stockwork veins. Their colors include purple, lilac, light green and colorless. The grain size varies from 1 to 10 mm. In the calcite-bearing pegmatite ore, fluorite occurs as irregular infilling, interstitial to grain of calcite and barite with colors of purple, lilac, light green and colorless and the size varying from 1 to 20 mm. In the thin-network aplite ores, fluorite is relatively rare, and occurs as purple, lilac and colorless veins with the size varying from 0.5 to 5 mm. Moreover, green, light green and colorless fluorite veins are also observed in the wallrocks with size of over 5 mm.

3 Samples and Analytical Methods

This paper presents the REE contents of fluorite, with various colors, collected from ores of all types in the Maoniuping REE deposit. For comparison, three fluorites with various colors from wallrocks were also measured for their REE contents. The sample was ground to 40 mesh in grain size, and fluorite grains of different colors were hand picked and separated using a binocular microscope. The selected fluorite sample was washed in 1: 10 acetic acid for 2 hours, then was cleaned in distilled water and dried, and finally, was ground to less than 200 mesh for analysis. Additionally, the REE contents of six syenites, eight carbonatites, three basalts, three rhyolites, and eighteen granites were analyzed. The REE contents were analyzed with ICP-MS techniques at the Institute of Geochemistry, Chinese Academy of Sciences following the procedure of Qi et al. (2000). The analytical error was less than 10%.

Sr-Nd data were analyzed at the Institute of Geology and Geophysics, Chinese Academy of Sciences. The analytical procedures are the same as described by Xu et al. (2003). The analytical result of standard sample NBS987 is $^{87}Sr/^{86}Sr$ = 0.710234±7 and La Jolla is $^{143}Nd/^{144}Nd$ = 0.511838±8. Pb data were analyzed at the Institute of Geochemistry, Chinese Academy of Sciences. The analytical procedures are the same as described by Xu et al. (2004). The analytical result of standard sample NBS981 is $^{206}Pb/^{204}Pb$ = 16.913±2, $^{207}Pb/^{204}Pb$ = 15.457±2, and $^{208}Pb/^{204}Pb$ = 36.611±4.

4 REE Contents and REE Patterns of Fluorite

The REE contents and chondrite-normalized REE patterns of fluorite in the Maoniuping REE deposit are given in Table 1 and Fig. 2 respectively. The REEs are subdivided into light REE (LREE: La, Ce, Pr, Nd), middle REE (MREE: Sm, Eu, Gd, Tb, Dy, Ho) and heavy REE (HREE: Er, Tm, Yb, Lu) for the purpose of describing and discussing the REE geochemistry of fluorite in the deposit. As can be seen from Table 1, there is no relationship either between the REE content of fluorite and the ore types in which it occurs, or between the REE content of fluorite and its color. Based on the REE patterns (Fig. 2), the fluorite in the orefield can be classified as the LREE-rich (Fig. 2a), LREE-flat (Fig. 2b, c, d) or LREE-depleted (Fig. 2e, f) types.

The range of total the REE contents (SREE) of the LREE-rich, LREE-flat and LREE-depleted fluorite in the deposit is from 338 to 667 ppm, 220 to 522 ppm and 248 to 464 ppm, respectively. From LREE-rich to LREE-flat to LREE-depleted fluorite, the LREE% (SLREE/SREE) tends to decrease and the MREE% (SMREE/SREE) and HREE% (SHREE/SREE) tend to increase (Table 2). In addition, from LREE-rich to LREE-flat to LREE-depleted fluorite, the Sm/Nd and La/Tb ratios tend to increase, but the Y/Ho ratios do not show any obvious variation (Table 2).

The REE patterns of the three types of fluorite in the deposit are obviously different (Fig. 2). The range of $(La/Sm)_N$ values of the LREE-rich, LREE-flat and LREE-depleted fluorite is from 1.99 to 3.37, 0.75 to 1.84 and 0.25 to 0.74, respectively (Table 2). From LREE-rich to LREE-flat to LREE-depleted fluorite, the $(La/Yb)_N$ values tend to decrease but the $(Gd/Yb)_N$ values show no obvious variation (Table 2). The REE patterns of the three types of fluorite show weakly negative Eu anomalies, but the ranges of the Eu/Eu* value of all types of fluorite are similar to each other (Table 2). The REE patterns of the LREE-rich fluorites show weakly negative Ce anomalies with Ce/Ce* values from 0.84 to 0.98, and the LREE-flat and LREE-depleted fluorite show weakly negative to weakly positive Ce anomalies with Ce/Ce* values from 0.83 to 1.08 and 0.99 to 1.08, respectively.

Table 1 and Fig. 2, the REE contents and REE patterns of fluorite in the wallrocks (Sample Nos. MNP-150, MNP-151 and MNP-151) are similar to those of the

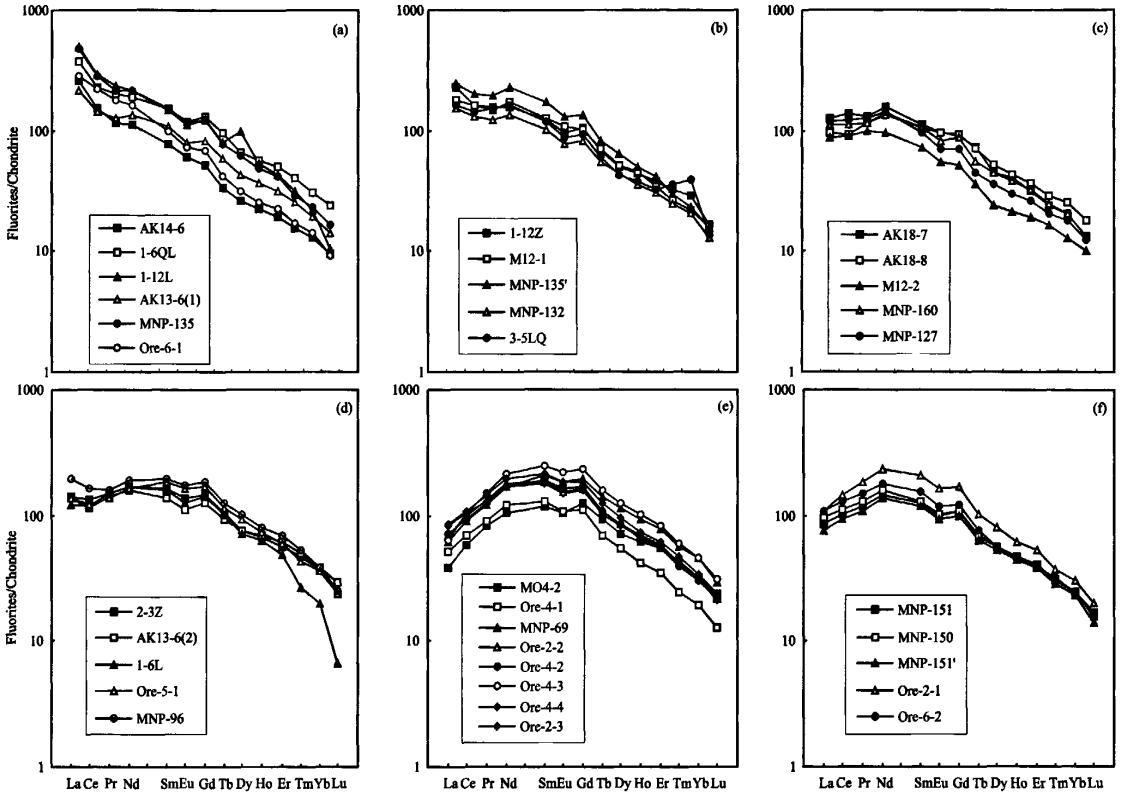

Fig. 2. The chondrite-normalized REE patterns of (a) LREE-rich fluorite, (b), (c) and (d) LREE-flat fluorite, (e) and (f) LREE-depleted fluorite. Sample Nos. are same as in Table 1 and the REE contents of chondrite are token from Boynton (1984).

LREE-depleted fluorite in the ores. This feature indicates that both types of fluorite in the orefield share a similar mechanism of formation.

5 Discussion

(1) REE contents and colors of fluorite

Several theories, including electron transition on structural defect center, impurity-associated defect center, and impurity ion, have been proposed to explain how the various colors occur in fluorite (Bill and Calas, 1978). The REE are important impurity elements in fluorite. Studies have indicated that the REE contents (especially Y) of fluorite are an important reason for color variations (Bill and Calas, 1978; Fayziyev, 1990; Chesley et al., 1991; Bühn et al., 2003). In summing up the REE geochemical characteristics of hydrothermal and magmatic fluorite from deposits in the former Soviet Union, Fayziyev (1990) found that the Y contents of dark-colored fluorite were higher than those of light-colored fluorite and the Y contents of green fluorite were higher than those of purple fluorite. Chesley et al. (1991) suggested that the colors of fluorite from the South Confty and Wheal Jane fluorite deposits in England were closely related to their Sm/Nd ratios. Bühn et al. (2003) found that from dark yellow, yellow, light yellow to colorless fluorite in a specimen from the Okorusu fluorite deposit in Namibia the REE contents tend to increase, but the REE patterns are similar.

In Fig. 3, the REE patterns of fluorite with different colors in a specimen from the Maoniuping REE deposit are similar to each other (Fig. 3a, b) and those of fluorite with the same color from the same ore type are obviously different (Fig. 3c, d). In Table 1, the Y contents of fluorite of different colors in the deposit vary in a wide range, and the Y content ranges of fluorite with different colors are mostly overlapping with each other. Besides, there is no correlation between Sm/Nd ratios and the color variations of fluorite (Table 1). Thus, the variations in the REE and Y contents of fluorite in this orefield are not responsible for their color changes.

(2) Genetic relationships among the three types of fluorite

In early-stage fluorite from the Maoniuping REE deposit, Niu et al. (1997) found fluid-melt inclusions, whose size varies from 15×15 to 100×100 mm, composed

Table 1 REE contents of the fluorite in Maoniuping REE deposit (ppm)

REE type	LREE-rich type		LREE-flat type						LREE-depleted type											
Sample No.	MNP-135	Ore-6-1	Ore-5-1	MNP-135'	MNP-132	MNP-127	MNP-96	MNP-160	Ore-4-1	Ore-4-2	Ore-4-3	Ore-4-4	Ore-2-1	Ore-2-2	Ore-2-3	Ore-6-2	MNP-69	MNP-151	MNP-150	MNP-151
Color	Colorless	Dark purple	Dark purple	Light purple	Light green	Green	Dark purple	Purple	Colorless	Purple	Green	Light purple	Green	Light purple	Purple	Light purple	Green	Light green	Colorless	Colorless
Ore type	B	T	B	B	B	C	T	T	B	B	B	B	C	C	C	T	T	F	F	F
La	148	88.2	43.1	75.7	47.4	36.9	61.2	34.3	16.0	22.4	19.6	26.2	33.2	21.3	25.9	33.2	19.2	26.6	29.5	23.4
Ce	231	177	97.9	163	105	99.3	133.4	89.6	55.6	75.9	84.7	88.5	118	80.5	83.8	104	74.0	82.4	90.1	75.0
Pr	26.3	21.5	16.6	24.1	14.9	15.4	19.5	14.1	11.2	15.3	18.3	17.6	22.3	16.0	15.6	18.4	14.9	14.4	15.7	13.3
Nd	129	98.0	99.8	137	80.6	85.2	113	81.0	73.0	102	130	117	139	106	102	108	102	86.8	94.5	81.2
Sm	29.8	19.3	36.1	34.0	20.0	18.8	38.7	20.8	25.2	37.3	48.9	41.9	40.6	35.7	34.7	30.3	40.1	24.5	25.3	23.1
Eu	8.60	5.37	12.0	9.71	5.73	5.13	12.7	6.12	7.94	11.9	16.3	13.5	12.0	11.5	11.1	8.80	13.4	7.30	7.46	6.85
Gd	32.0	17.7	43.7	35.1	21.5	18.5	47.4	22.6	29.0	43.8	60.9	48.3	44.0	42.0	41.1	32.0	51.0	27.7	28.1	25.9
Tb	3.69	1.98	5.41	3.90	2.60	2.09	5.88	2.58	3.32	5.16	7.51	5.90	4.90	5.08	4.87	3.57	6.62	3.20	3.29	3.02
Dy	20.1	10.3	29.8	21.0	14.1	11.6	32.6	14.4	17.8	27.6	40.3	31.2	26.2	27.7	27.1	18.0	37.3	18.4	18.2	17.0
Ho	3.49	1.85	5.28	3.57	2.58	2.16	5.74	2.70	3.04	4.75	7.26	5.33	4.43	4.92	4.81	3.33	6.78	3.35	3.39	3.21
Er	8.85	4.77	12.6	8.89	6.51	5.56	14.7	6.85	7.32	11.7	17.2	12.9	11.1	12.2	12.0	8.02	16.4	8.66	8.35	8.15
Tm	0.93	0.55	1.42	0.96	0.79	0.67	1.71	0.80	0.81	1.26	1.92	1.51	1.20	1.35	1.34	1.03	1.85	0.99	1.02	0.93
Yb	4.92	3.00	7.64	4.87	4.31	3.75	8.09	4.34	4.05	6.36	9.56	7.09	6.26	6.80	6.56	5.01	9.59	5.06	5.15	4.83
Lu	0.54	0.31	0.78	0.52	0.44	0.41	0.85	0.44	0.43	0.72	1.03	0.79	0.66	0.72	0.70	0.53	0.99	0.52	0.55	0.47
Y	237	133	379	232	194	175	430	218	211	340	527	376	320	350	343	233	477	263	272	248
ΣREE	647	450	412	522	326	305	495	301	255	366	463	418	464	372	372	374	394	310	331	286
ΣLREE	534	385	257	400	248	237	327	219	156	216	253	249	313	224	227	264	210	210	230	193
ΣMREE	97.7	56.5	132	107	66.5	58.3	143	69.2	86.3	131	181	146	132	127	124	96.0	155	84.5	85.7	79.1
ΣHREE	15.2	8.63	22.4	15.2	12.1	10.4	25.4	12.4	12.6	20.0	29.7	22.3	19.2	21.1	20.6	14.6	28.8	15.2	15.1	14.4
LREE%	82.55	85.52	62.46	76.54	75.94	77.52	66.02	72.85	61.17	58.88	54.50	59.68	67.37	60.20	61.17	70.45	53.31	67.83	69.51	67.36
MREE%	15.09	12.56	32.10	20.54	20.37	19.08	28.87	23.02	33.88	35.64	39.09	34.98	28.49	34.13	33.28	25.66	39.38	27.25	25.93	27.62
HREE%	2.35	1.92	5.44	2.92	3.69	3.40	5.12	4.13	4.95	5.47	6.41	5.34	4.14	5.67	5.54	3.90	7.31	4.91	4.56	5.02
Sm/Nd	0.23	0.20	0.36	0.25	0.25	0.22	0.34	0.26	0.35	0.37	0.38	0.36	0.29	0.34	0.34	0.28	0.39	0.28	0.27	0.28
Tb/La	0.025	0.022	0.125	0.052	0.055	0.057	0.096	0.075	0.208	0.230	0.383	0.225	0.147	0.238	0.188	0.108	0.345	0.120	0.111	0.129
Y/Ho	67.93	72.06	71.85	64.99	75.28	81.28	75.04	80.64	69.50	71.63	72.53	70.62	72.32	71.12	71.30	69.81	70.35	78.47	80.01	77.34
Eu/Eu*	0.85	0.89	0.93	0.86	0.85	0.84	0.91	0.86	0.90	0.90	0.91	0.92	0.87	0.90	0.90	0.86	0.91	0.86	0.86	0.86
Ce/Ce*	0.89	0.98	0.88	0.92	0.95	1.00	0.93	0.98	1.00	0.99	1.08	0.99	1.04	1.05	1.00	1.01	1.05	1.01	1.01	1.02
$(La/Sm)_N$	3.11	2.88	0.75	1.40	1.49	1.24	1.00	1.04	0.40	0.38	0.25	0.39	0.51	0.38	0.47	0.69	0.30	0.68	0.74	0.64
$(La/Yb)_N$	20.20	19.81	3.81	10.49	7.42	6.63	5.10	5.32	2.66	2.38	1.38	2.49	3.58	2.12	2.66	4.47	1.35	3.54	3.87	3.27
$(Gd/Yb)_N$	5.24	4.75	4.61	5.82	4.02	3.99	4.72	4.19	5.77	5.56	5.14	5.49	5.67	4.99	5.05	5.15	4.29	4.41	4.40	4.33
Data source	This paper																			

(continued)

REE type	LREE-rich type				LREE-flat type									LREE-depleted type
Sample No.	AK13-6(1)	AK14-6	1-6QL	1-12L	AK18-8	AK18-7	AK13-6(2)	M12-1	M12-2	1-6L	2-3Z	1-12Z	3-5LQ	MO4-2
Color	Purple	Colorless			Purple	Light green	Colorless	Purple	Light green					Light green
Ore type	B	C	B	B	B	B	B	C	C	B	B	B	B	B
La	66.1	80.8	115	150	29.5	39.9	42.1	54.4	27.5	37.9	44.2	70.7	49.6	11.7
Ce	115	123	185	238	76.2	113	91.8	130	72.4	96.3	108	131	117	47.6
Pr	15.5	14.1	24.3	28.6	14.3	15.7	17.1	18.1	12.2	18.1	18.5	19.1	18.9	10.2
Nd	79.6	68.1	112	127	83.6	94.9	94.5	103	57.8	100	100	93.7	96.2	62.4
Sm	20.9	15.1	29.3	29.0	20.8	22.0	26.9	24.9	14.3	30.7	31.8	24.2	23.2	22.9
Eu	5.83	4.49	8.62	8.25	7.02	6.95	8.21	8.02	4.04	9.25	10.1	6.97	6.48	7.82
Gd	21.4	13.6	33.9	31.8	24.2	23.1	32.9	26.6	13.5	36.9	37.9	26.9	23.9	32.7
Tb	2.81	1.61	4.55	3.82	3.35	3.40	4.42	3.30	1.70	4.84	4.97	3.20	2.87	4.43
Dy	13.7	8.48	21.3	31.8	16.6	14.5	24.4	16.6	7.83	23.0	24.3	16.3	13.8	23.1
Ho	2.62	1.59	4.13	3.82	3.13	2.93	4.96	3.29	1.54	4.57	4.85	3.22	2.69	4.46
Er	6.63	4.05	10.5	8.96	7.76	6.54	13.1	7.34	4.02	10.3	11.7	7.95	6.79	11.5
Tm	0.84	0.51	1.31	1.04	0.95	0.77	1.64	0.84	0.54	0.87	1.52	1.05	1.16	1.41
Yb	4.08	2.72	6.40	4.52	5.27	4.26	8.01	4.51	2.73	4.22	7.89	5.96	8.17	6.77
Lu	0.47	0.32	0.79	0.35	0.61	0.45	0.97	0.54	0.33	0.22	0.80	0.55	0.45	0.80
Y	217	126	353	306	272	226	475	254	145	361	394	264	232	398
ΣREE	355	338	557	667	293	348	371	401	220	377	407	411	371	248
ΣLREE	276	286	436	544	204	264	246	306	170	252	271	315	282	132
ΣMREE	67.3	44.9	102	108	75.1	72.9	102	82.7	42.9	109	114	80.8	72.9	95.4
ΣHREE	12.0	7.60	19.0	14.9	14.6	12.0	23.7	13.2	7.6	15.6	21.9	15.5	16.6	20.5
LREE%	77.70	84.50	78.32	81.50	69.42	75.63	66.17	76.10	77.08	66.89	66.59	76.56	75.89	53.23
MREE%	18.92	13.26	18.27	16.27	25.61	20.92	27.44	20.60	19.47	28.97	28.02	19.67	19.65	38.50
HREE%	3.38	2.25	3.41	2.23	4.97	3.45	6.39	3.30	3.46	4.14	5.39	3.78	4.46	8.27
Sm/Nd	0.26	0.22	0.26	0.23	0.25	0.23	0.28	0.24	0.25	0.31	0.32	0.26	0.24	0.37
Tb/La	0.043	0.020	0.040	0.025	0.114	0.085	0.105	0.061	0.062	0.128	0.113	0.045	0.058	0.378
Y/Ho	82.80	79.10	85.48	80.20	86.74	77.08	95.88	77.17	94.04	78.87	81.43	81.93	86.10	89.12
Eu/Eu*	0.84	0.96	0.84	0.83	0.96	0.94	0.84	0.95	0.89	0.84	0.89	0.84	0.84	0.87
Ce/Ce*	0.86	0.88	0.84	0.87	0.89	1.08	0.83	1.00	0.95	0.89	0.91	0.86	0.92	1.05
$(La/Sm)_N$	1.99	3.37	2.46	3.26	0.89	1.14	0.98	1.38	1.21	0.78	0.87	1.84	1.34	0.32
$(La/Yb)_N$	10.91	20.01	12.10	22.41	3.77	6.31	3.54	8.15	6.79	6.06	3.77	7.99	4.09	1.17
$(Gd/Yb)_N$	4.23	4.03	4.27	5.67	3.71	4.37	3.31	4.76	3.99	7.05	3.88	3.64	2.36	3.89
Data source	Yuan et al. (1995)		Niu et al. (1996)		Yuan et al. (1995)					Niu et al. (1996)				Yuan et al. (1995)

Note: LREEs include La, Ce, Pr and Nd, MREEs include Sm, Eu, Gd, Tb, Dy and Ho and HREEs include Er, Tm, Yb and Lu. LREE% – ΣLREE/ΣREE, MREE% – ΣMREE/ΣREE, and HREE% – ΣHREE/ΣREE. Ore type B is barite-bearing pegmatite, C – calcite-bearing pegmatite, T – thin-network aplite and F – fluorite in the wallrocks.

Table 2 The comparison of REE geochemistry of fluorite and various magmatic rocks in the Maoniuping REE deposit

Fluorite or Rock	Fluorite			Carbonatite	Syenite	Granite	Rhyolite	Basalt
	LREE-rich type	LREE-flat type	LREE-depleted type					
$N^{\#}$	6	15	13	8	6	18	3	3
La	108 (66.1–150)	46.3 (27.5–75.7)	23.7 (11.7–33.2)	628 (454–828)	334 (127–945)	49.06 (23.9–95.4)	33.77 (16.9–48.8)	26.4 (20.6–38.0)
Ce	178 (115–238)	108 (72.4–163)	81.5 (47.6–118)	1330 (916–1730)	501 (119–1604)	94.59 (44.9–159)	55.93 (42.6–66.2)	54.4 (41.4–78.1)
Pr	21.7 (14.1–28.6)	17.1 (12.2–24.1)	15.6 (10.2–22.3)	134 (94.7–176)	48.8 (15.9–153)	10.00 (4.62–17.4)	6.05 (3.03–8.41)	6.54 (4.77–8.9)
Nd	102 (68.1–129)	94.7 (57.8–137)	100 (62.4–139)	526 (377–687)	151 (49.1–481)	34.05 (15.1–57.4)	19.7 (8.95–27.6)	25.6 (17.8–33.3)
Sm	23.9 (15.1–29.8)	25.8 (14.3–38.7)	33.1 (22.9–48.9)	78.7 (63.5–99.5)	17.3 (7.36–52.7)	6.86 (3.35–11.5)	3.87 (2.15–4.82)	5.76 (3.92–6.8)
Eu	6.86 (4.49–8.62)	7.90 (4.04–12.7)	10.5 (6.85–16.3)	17.3 (14.4–21.0)	3.77 (1.81–11.1)	0.66 (0.28–1.24)	0.58 (0.24–0.7)	1.65 (1.23–2.16)
Gd	25.1 (13.6–33.9)	29.0 (13.5–47.4)	39.0 (25.9–60.9)	54.7 (45.5–65.6)	10.1 (5.21–29.3)	6.51 (3.38–11.03)	3.51 (2.41–4.14)	5.78 (4.20–7.49)
Tb	3.08 (1.61–4.55)	3.63 (1.7–5.88)	4.68 (3.02–7.51)	6.27 (5.20–7.33)	1.20 (0.65–3.23)	1.18 (0.64–2.33)	0.62 (0.52–0.66)	0.97 (0.72–1.23)
Dy	17.6 (8.48–31.8)	18.7 (7.83–32.6)	25.4 (17.0–40.3)	29.4 (24.4–33.2)	5.36 (2.83–12.9)	7.24 (3.77–14.76)	4.03 (3.64–3.96)	5.55 (4.13–7.47)
Ho	2.92 (1.59–4.13)	3.55 (1.54–5.74)	4.54 (3.04–7.26)	5.0 (4.16–5.68)	0.91 (0.44–1.96)	1.51 (0.76–3.10)	0.88 (0.82–0.88)	1.15 (0.89–1.46)
Er	7.29 (4.05–10.5)	8.71 (4.02–14.7)	11.2 (7.32–17.2)	15.0 (12.7–17.3)	2.34 (1.06–4.59)	4.42 (2.24–9.27)	2.53 (2.44–2.62)	3.12 (2.47–3.88)
Tm	0.86 (0.51–1.31)	1.05 (0.54–1.71)	1.28 (0.81–1.92)	1.90 (1.53–2.38)	0.33 (0.14–0.55)	0.72 (0.36–1.48)	0.43 (0.38–0.47)	0.47 (0.39–0.56)
Yb	4.27 (2.72–6.4)	5.60 (2.73–8.17)	6.39 (4.05–9.59)	12.2 (10.1–15.7)	2.16 (0.94–3.58)	5.12 (2.74–10.36)	3.18 (2.72–3.57)	3.19 (2.63–3.77)
Lu	0.46 (0.31–0.79)	0.56 (0.22–0.97)	0.69 (0.43–1.03)	1.51 (1.24–2.03)	0.29 (0.11–0.53)	0.73 (0.43–1.39)	0.48 (0.43–0.54)	0.45 (0.36–0.54)
Y	229 (126–353)	283 (145–475)	335 (211–527)	146 (131–157)	27.1 (15.8–52.2)	46.0 (24.2–89.4)	25.3 (24.1–26.5)	31.6 (25.3–39.6)
ΣREE	502 (338–667)	371 (220–522)	358 (248–464)	2840 (2051–3651)	1079 (340–3303)	223 (107–371)	136 (87.9–173)	141 (106–186)
ΣLREE	410 (276–544)	267 (170–400)	221 (132–313)	2618 (1842–3387)	1035 (311–3183)	188 (89.3–329)	115 (71.5–151)	113 (84.6–158)
ΣMREE	79.4 (44.9–108)	88.6 (42.9–143)	117 (79.1–181)	191 (157–232)	38.7 (20.5–111)	23.96 (12.2–43.4)	13.50 (9.78–15.6)	20.9 (15.1–26.6)
ΣHREE	12.9 (7.60–19.0)	15.9 (7.60–25.4)	19.5 (12.6–29.7)	30.7 (25.6–37.4)	5.12 (2.25–8.43)	10.99 (5.77–22.5)	6.62 (6.07–7.20)	7.23 (5.85–8.75)
LREE%	81.68 (77.7–85.52)	72.11 (62.46–77.52)	61.90 (53.23–70.45)	91.99 (89.79–93.15)	95.16 (91.49–96.68)	84.29 (80.75–88.71)	84.53 (81.36–87.10)	79.40 (73.07–84.97)
MREE%	15.73 (12.56–18.92)	23.62 (19.08–32.1)	32.60 (25.66–39.38)	6.88 (5.92–8.39)	4.11 (2.63–6.45)	10.80 (7.97–12.72)	10.19 (8.74–11.13)	15.26 (11.22–20.27)
HREE%	2.59 (1.92–3.41)	4.27 (2.92–6.39)	5.50 (3.90–8.27)	1.13 (0.87–1.82)	0.73 (0.26–2.07)	4.91 (3.32–6.58)	5.28 (4.15–7.51)	5.34 (3.81–6.66)
Sm/Nd	0.23 (0.20–0.26)	0.27 (0.22–0.36)	0.33 (0.27–0.39)	0.15 (0.14–0.17)	0.12 (0.09–0.15)	0.20 (0.17–0.22)	0.21 (0.17–0.24)	0.23 (0.20–0.27)
Y/Ho	77.93 (67.93–85.48)	80.55 (64.99–95.88)	74.16 (69.50–89.12)	29.57 (27.46–31.49)	31.42 (26.63–36.12)	30.72 (28.43–33.28)	28.77 (26.81–30.11)	27.53 (27.03–28.43)
Eu/Eu*	0.87 (0.83–0.96)	0.88 (0.84–0.96)	0.89 (0.86–0.92)	0.80 (0.78–0.81)	0.89 (0.63–1.01)	0.32 (0.16–0.43)	0.45 (0.32–0.57)	0.87 (0.78–0.92)
Ce/Ce*	0.89 (0.84–0.98)	0.93 (0.83–1.08)	1.02 (0.99–1.08)	1.10 (1.06–1.16)	0.88 (0.64–1.02)	1.02 (0.74–1.16)	1.05 (0.79–1.43)	0.99 (0.95–1.02)
$(La/Sm)_N$	2.85 (1.99–3.37)	1.16 (0.75–1.84)	0.47 (0.25–0.74)	4.98 (4.27–6.17)	12.55 (9.65–20.01)	4.58 (3.46–6.29)	5.38 (4.83–6.37)	2.95 (1.91–3.64)
$(La/Yb)_N$	17.57 (10.91–22.41)	5.95 (3.54–10.49)	2.69 (1.17–4.47)	35.11 (19.50–44.30)	112.01 (26.51–213.80)	6.78 (4.12–11.09)	7.18 (3.50–9.22)	5.68 (3.70–8.06)
$(Gd/Yb)_N$	4.70 (4.03–5.67)	4.29 (2.36–7.05)	4.93 (3.89–5.77)	3.64 (2.52–4.19)	4.18 (1.42–7.93)	1.05 (0.79–1.20)	0.91 (0.60–1.18)	1.44 (1.29–1.60)

The primary data of fluorites after Table 1, various magmatic rocks after Appendix. $N^{\#}$ is the sample number. The figure in front of brackets is the average and that in brackets the range.

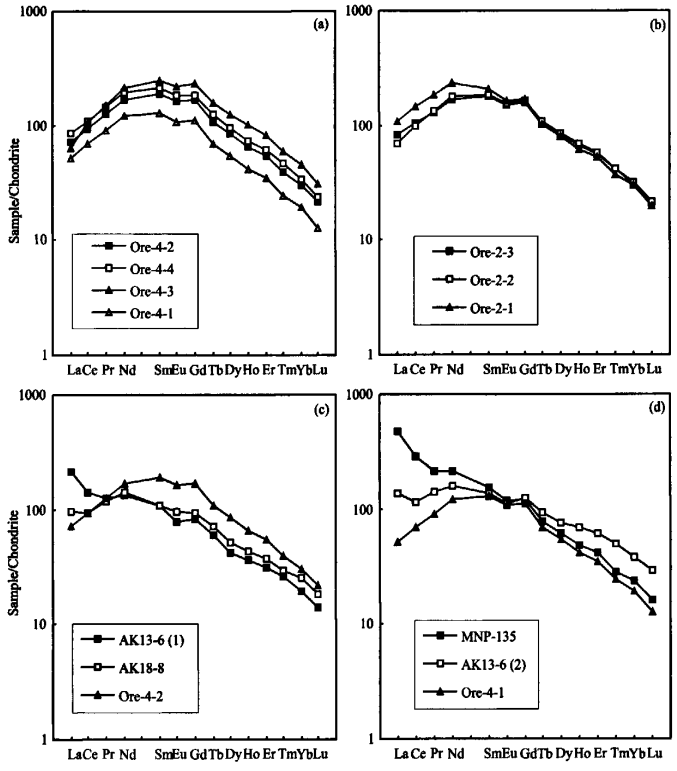

Fig. 3. The chondrite-normalized REE patterns of (a) different colors fluorite from a specimen of barite-bearing pegmatite ore, (b) fluorite with different colors from a specimen of calcite-bearing pegmatite ore, (c) purple fluorite from barite-bearing pegmatite ore, and (d) colorless fluorite from barite-bearing pegmatite ore. The REE contents of chondrite are token from Boynton (1984).

of vapor phase (5% to 10%), liquid phase (5% to 35%) and crystal phase (60% to 90%), salinity varies mostly from 10.3% to 13.1%, and homogenization temperatures (T_h) varies from 452°C to 502°C. Hence, Niu et al. (1997) suggested that these fluorites were crystallized from F-rich salt melts of magmatic origin. Yuan et al. (1995) determined the T_h of daughter crystal-bearing multiphase inclusions and gas-fluid-CO_2 three-phase inclusions in fluorite of 360°C to 410°C and 328°C to 376°C, respectively. These features show that fluorite in the deposit was formed at relatively high temperatures. In addition, Yuan et al. (1995) reported that the $(^{87}Sr/^{86}Sr)_0$ value of one fluorite sample in the deposit is 0.70637. Huang et al. (2003) analyzed the $(^{87}Sr/^{86}Sr)_0$ and $(^{143}Nd/^{144}Nd)_0$ values of six fluorite samples in the deposit, varying from 0.706027 to 0.706237 and 0.512370 to 0.512412, respectively (Table 3). All of samples are plotted into the narrow range between EM1 and EM2 in the Epsilon Nd vs $(^{87}Sr/^{86}Sr)_0$ diagram (Fig. 4). Hence, the fluorite in the Maoniuping REE deposit can be considered to be of magmatic origin. Based on the REE geochemistry, the fluorite in the deposit is considered to be the product of the same sourced fluids at different stages.

(a) Bau and Dulski (1995) studied REE geochemistry of fluorite from the Tannenboden and Beihilfe deposits in Germany, and proposed that the horizontal distribution of fluorites plotted in the Y/Ho vs La/Ho diagram showed that they were formed from the same source. Figure 5 shows that all fluorite in the deposit display the above feature, implying that they were formed from the same source. In Table 3, the Sr, Nd and Pb isotopic compositions of three types of fluorite in the deposit do not have obvious difference and it also confirms that they were formed from the same source.

(b) After studying the REE variations of fluorites formed through the ore-forming process, Möller et al. (1976) found that the early fluorite is relatively enriched in LREE while the late fluorite is enriched in HREE, and the

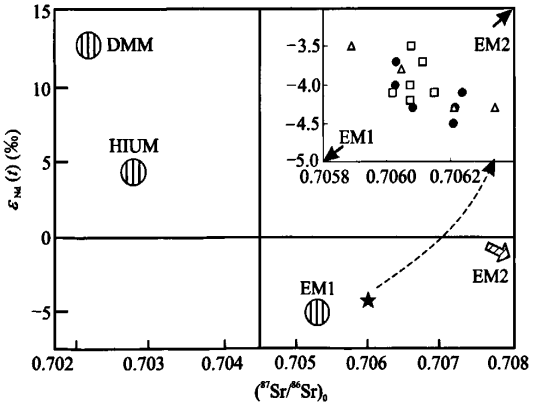

Fig. 4. The Epsilon Nd vs $(^{87}Sr/^{86}Sr)_0$ diagram of fluorite (●), carbonatite (□) and syenite (△). DMM, HIUM, EM1 and EM2 after Zindler and Hart (1986).

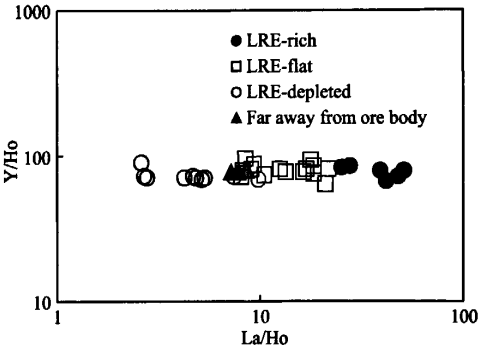

Fig. 5. The Y/Ho vs La/Ho diagram of fluorite.

Table 3 The Sr, Nd and Pb isotopic compositions of fluorites and rocks in the Mianning REE deposit

Sample No.	Fluorite or Rock	$^{87}Rb/^{86}Sr$	$^{87}Sr/^{86}Sr$	$(^{87}Sr/^{86}Sr)_0$	Epsilon Sr	$^{147}Sm/^{144}Nd$	$^{143}Nd/^{144}Nd$	$(^{143}Nd/^{144}Nd)_0$	Epsilon Nd	$^{206}Pb/^{204}Pb$	$^{207}Pb/^{204}Pb$	$^{208}Pb/^{204}Pb$
Ore-6-1	LRE-rich Fluorite	3.25E-05	0.706031	0.706031	22.2	0.0951	0.512431	0.512412	−3.7	18.323	15.586	38.405
MNP-135	LRE-rich Fluorite	6.35E-05	0.706213	0.706213	24.8	0.1544	0.512409	0.512379	−4.3	18.458	15.632	38.285
MNP-127	LRE-flat Fluorite	3.13E-04	0.706027	0.706027	22.2	0.1287	0.512422	0.512397	−4.0	18.177	15.536	38.386
Ore-5-1	LRE-flat Fluorite	7.96E-05	0.706208	0.706208	24.7	0.2199	0.512413	0.512370	−4.5	18.557	15.549	38.290
MNP-69	LRE-depleted Fluorite	1.83E-05	0.706237	0.706237	25.2	0.2377	0.512437	0.512390	−4.1	18.241	15.538	38.331
MNP-151	LRE-depleted Fluorite	2.62E-05	0.706084	0.706084	23.0	0.1586	0.512412	0.512381	−4.3	18.246	15.559	38.391
MNP-10	Carbonate	2.14E-05	0.706075	0.706075	22.8	0.0888	0.512414	0.512397	−4.0	17.887	15.362	38.141
MNP-13	Carbonate	8.55E-04	0.706020	0.706020	22.1	0.0836	0.512405	0.512389	−4.1	18.223	15.538	38.323
MNP-15-1	Carbonate	1.21E-04	0.706079	0.706079	23.0	0.0837	0.512436	0.512420	−3.5	18.417	15.429	38.233
MNP-16	Carbonate	5.40E-05	0.706075	0.706075	22.8	0.1001	0.512405	0.512385	−4.2	18.264	15.556	38.683
MNP-125	Carbonate	5.19E-05	0.706149	0.706149	23.9	0.0983	0.512411	0.512392	−4.1	18.220	15.587	38.452
MNP-135	Carbonate	7.32E-05	0.706074	0.706074	22.8	0.0946	0.512411	0.512392	−4.0			
MNP-142	Carbonate	9.54E-05	0.706113	0.706113	23.4	0.0943	0.512427	0.512409	−3.7	18.001	15.435	38.083
MNP-15	Syenite	1.77	0.706796	0.706047	22.5	0.0780	0.512422	0.512407	−3.8	18.270	15.648	38.611
MNP-24	Syenite	0.897	0.706719	0.706340	26.6	0.0588	0.512391	0.512379	−4.3	18.263	15.694	38.788
MNP-42	Syenite									18.259	15.605	38.496
MNP-54	Syenite									18.356	15.613	38.592
MNP-65	Syenite									18.437	15.605	38.590
MNP-70	Syenite	1.17	0.706383	0.705888	20.2	0.0869	0.512436	0.512419	−3.5			
MNP-88	Syenite	1.54	0.706863	0.706211	24.8	0.0568	0.512391	0.512380	−4.3	18.465	15.657	38.685
MNP-78	Granite	4.97	0.744440	0.726017	449	0.1161	0.512494	0.512403	−1.6	18.982	15.592	38.953
MNP-42	Granite	10.6	0.743765	0.725747	304	0.0619	0.512419	0.51237	−2.2			
MNP-50	Granite									19.103	15.627	39.194
MNP-30	Granite									18.996	15.617	39.168
MNP-51	Granite									19.022	15.595	39.005

Isotope results normalized to $^{146}Nd/^{144}Nd=0.7219$ and $^{86}Sr/^{86}Sr=0.1194$. $(^{87}Sr/^{86}Sr)_0$, $(^{143}Nd/^{144}Nd)_0$, Epsilon Sr and Epsilon Nd values of fluorite, carbonatie and syenite are calculated for t = 30 Ma, granites for t =100 Ma. The Sr, Nd and Pb isotopic compositions of granite are analyzed in this study, Sr and Nd isotopic compositions of fluorite after Huang et al. (2003), carbonatie and syenite after Xu et al. (2003), Pb isotopic compositions of fluorite, carbonatie and syenite after Xu et al. (2004).

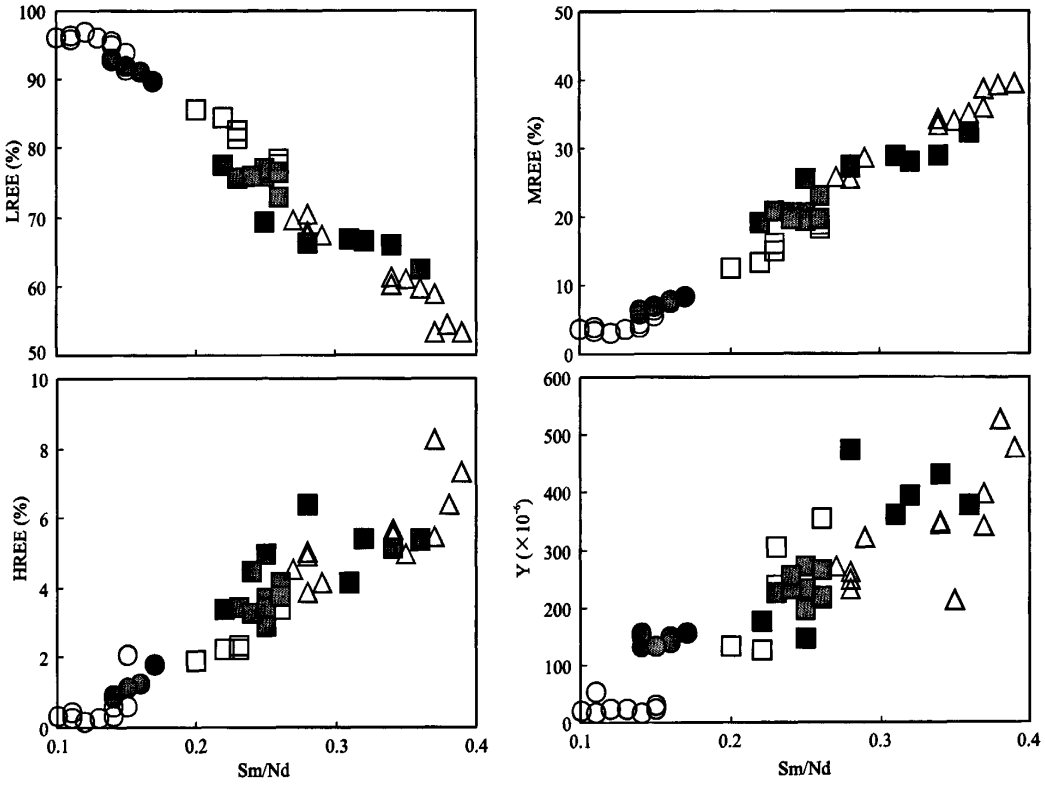

Fig. 6. The correlation diagram between the Sm/Nd ratio and the percentage of REE groups and Y contents of LREE-rich fluorite (□), LREE-flat fluorite (■), LREE-depleted fluorite (△), carbonatite (●) and syenite (○).

Tb/La ratios in the former are lower than those in the latter. Chesley et al. (1991) also found that there is REE fractionation through the formation process of fluorite, with early fluorite higher in LREE and lower in Sm/Nd ratios than the late fluorite. Using the Tb/La ratios of fluorite from south-central Idaho, U.S., Constantopoulos (1988) discussed the variations of REE contents of fluorite through the ore-forming stages and suggested that early fluorite were relatively rich in La, poorer in Tb and lower in Tb/La ratios than the late fluorite. The data of Bühn et al. (2002, 2003) also show that the early fluorite from the Okorusu fluorite deposit in Namibia is relatively rich in LREE and lower in Tb/La ratios than late fluorite. McLennan and Taylor (1979), Wood (1990) and Bau and Dulski (1995) suggested that REE in the hydrothermal system are normally carried in the form of F-complexes, whose stability decreases from LREE to MREE to HREE (including Y). In the process of formation of fluorites, with decreasing F content in the fluids, the LREE in the fluids would decrease relatively but MREE and HREE would increase. Therefore, the early fluorite is relatively enriched in LREE and the late fluorite enriched in MREE and HREE.

As can be seen from Table 1, the LREE contents decrease gradually but the MREE contents, HREE contents, Sm/Nd ratios and Tb/La ratios increase from LREE-rich to LREE-flat to LREE-depleted fluorite. Figure 6 also shows that there are negative correlations between the Sm/Nd ratios and the LREE%, but positive correlations between the Sm/Nd ratios and the MREE%, HREE% and Y contents. These indicate that the three types of fluorite in the Maoniuping REE deposit were formed at different stages, with the LREE-rich fluorite forming in the early, the LREE-flat fluorite forming in the middle and the LREE-depleted fluorite forming in the late stage.

(3) The source of ore-forming fluids

Although many previous studies suggested that the mineralization of the Maoniuping REE deposit is related to alkaline magmatism (syenite-carbonatite) (Pu, 1993; Niu and Lin, 1994; Yuan et al., 1995), the source of the ore-forming fluids is still debated. Fluorite is one of the main gangue minerals in the Maoniuping REE deposit. In the deposit, fluorite occurs not only in ores of various types, but also in wallrocks outside the orebodies.

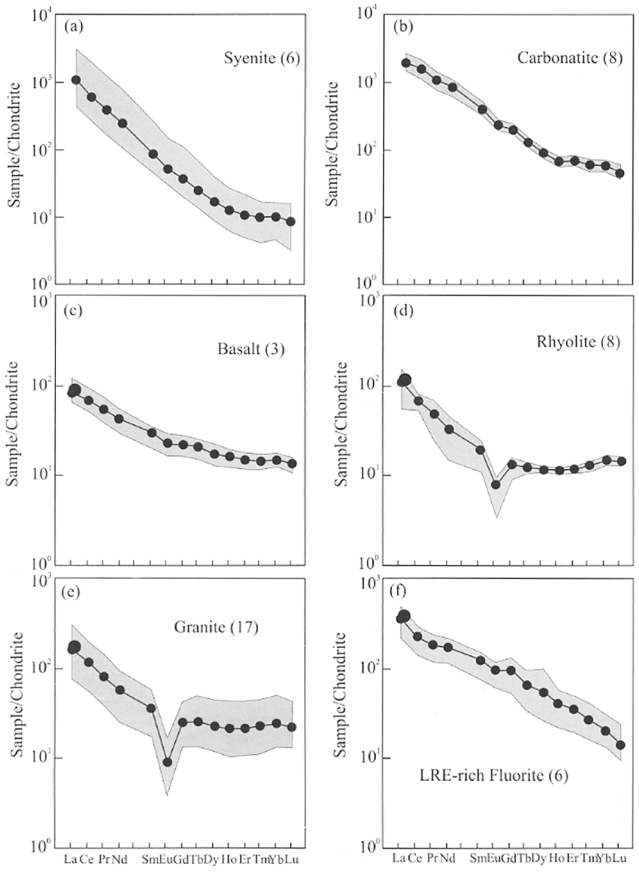

Fig. 7. The chondrite-normalized REE patterns of (a) syenite, (b) carbonatite, (c) basalt, (d) rhyolite, (e) granite, and (f) LREE- rich fluorite. The shadowed field and solid circle line are the range and average value of REE, respectively. The figure in brackets is the sample number. The REE contents of chondrite are token from Boynton (1984).

Moreover, the REE patterns of fluorite in wallrocks are similar to those of the LREE-depleted fluorite (late stage) in the orebody (Table 1, Fig. 2). This means that the formation of fluorite in this region occurs throughout the whole process of mineralization. Therefore, the REE geochemistry of fluorite in the orefield records important information about the source of ore-forming fluids.

Figure 7 shows that the REE patterns of the early fluorite (LREE-rich type) are similar to those of syenite and carbonatite, but different from those of basalt, rhyolite and granite in the orefield. In Table 2 one can see that the range of the $(La/Nd)_N$, $(Gd/Yb)_N$ and Eu/Eu* values of the early fluorite are close to those of syenite and carbonatite but different from those of basalt, rhyolite and granite in the orefield. In Fig. 6, there is a good evolutionary trend from syenite and carbonatite to the three types of fluorite. These features show that the mineralization of the Maoniuping REE deposits is related to carbonatite-syenite magmatism and the ore-forming fluids are mainly derived from carbonatite and syenite melts. This conclusion is supported by the following evidence.

(a) Syenite and carbonatite in the Maoniuping REE deposits are closely related to REE mineralization in time and space. In space, the syenite and carbonatite are the main host rocks and the distribution of the two types of rock and the orebodies are controlled by the NE Haha fault zone (Fig. 1). In time, the two types of rock and REE mineralization are Himalayan in age. Yuan et al. (1995) reported that the K-Ar ages of syenite and carbonatite in the deposit were from 28 to 48 Ma and 31.7±0.7 Ma, respectively, and the isotopic ages of arfvedsonite and biotite gangue minerals in ores were 23 Ma and from 27 to 40±0.7 Ma, respectively.

(b) The REE contents of carbonatite (SREE from 2051 to 3651 ppm) and syenite (SREE from 340 to 3303 ppm) in the orefield are obviously higher than those of basalt (SREE from 106 to 186 ppm), rhyolite (SREE from 87.9 to 173 ppm) and granite (SREE from 107 to 371 ppm) in this area (Table 2). It is shown that carbonatite and syenite in the orefield have the potential of providing ore-forming materials. Studies have indicated that the LREE-rich fluids could be separated from the silicate-carbonatite magmatic system in the process of evolution (Wendlandt and Harrison, 1979; Ngwenya, 1994; Bulakh et al., 2000; Nasraoui et al., 2000; Groves and Vielreicher, 2001; Zaitsev et al., 2002). In Fig. 8, the $^{206}Pb/^{204}Pb$, $^{207}Pb/^{204}Pb$ and $^{208}Pb/^{204}Pb$ ratios of fluorite, pyrite and galena in the orefield are similar to those of carbonatite and syenite, but are apparently different from those of granites in the Yanshanian period in this area. It also shows that the ore-forming materials might mainly originate from carbonatites and syenites. In Table 3 and Fig. 5, the $(^{87}Sr/^{86}Sr)_0$ of fluorite (from 0.70603 to 0.70624) in the orefield are close to those of carbonatite (from 0.70602 to 0.70615) and syenite (from 0.70589 to 0.70634), but is obviously different from that of granite (from 0.72575 to 0.73602). It proves that the ore-forming materials mainly originated from carbonatite and syenite,

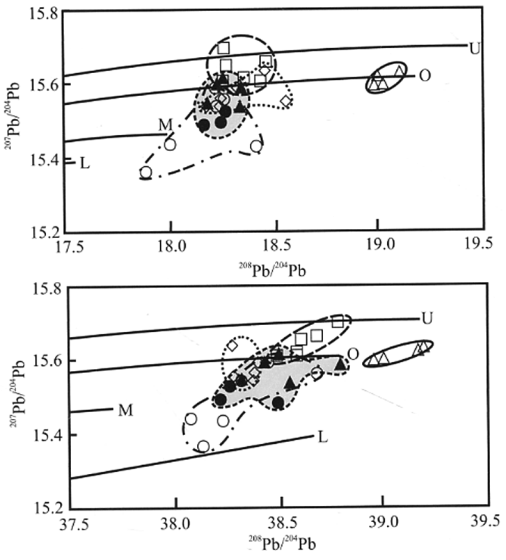

Fig. 8. The $^{207}Pb/^{204}Pb$ vs $^{206}Pb/^{204}Pb$ (A) and $^{207}Pb/^{204}Pb$ vs $^{208}Pb/^{204}Pb$ diagram of fluorite (◇), carbonatite (○), syenite (□), granite (△), pyrite (▲) and galena (●). Pb isotopic compositions of pyrite and galena come from Yuan et al. (1995), other data from Table 3. The evolutionary line of the upper crust (U), orogenic belt (O), mantle (M) and lower crust (L) after Zartman and Doe (1981).

too.

(c) Because the REE of fluorite mainly originated from REE-F complexes of ore-forming fluid (McLennan and Taylor, 1979; Wood, 1990; Bau and Dulski, 1995), the Nd isotopic compositions of fluorite are very important to trace the sources of REE and F of ore-forming fluids. As can be seen from Table 3 and Fig. 4, the $(^{143}Nd/^{144}Nd)_0$ of fluorite (from 0.512370 to 0.512412) also are close to that of carbonatite (from 0.512385 to 0.512420) and syenite (from 0.512379 to 0.512419). These suggest that the REE and F of ore-forming fluids mainly came from these two kinds of rock. Additionally, it is confirmed by many investigations that carbonatite magma can differentiate F-rich fluids (Deans and Powell, 1968; Gittins, 1989; Jago and Gittins, 1991; Simonetti and Bell, 1995).

(d) Yuan et al. (1995) reported the $\delta^{13}C_{PDB}$ and $\delta^{18}O_{SMOW}$ values of seven gangue calcites in the Maoniuping REE deposit varying from −6.3‰ to −6.8‰ and 7.0‰ to 7.8‰, respectively, which are close to those of the eight carbonatite samples in the orefield of Xu et al. (2003) ($\delta^{13}C_{PDB}$ from −6.6‰ to −7.0‰ and $\delta^{18}O_{SMOW}$ from 6.4‰ to 7.4‰) and are within the respective ranges of the $\delta^{13}C_{PDB}$ (−4‰ to −8‰) and $\delta^{18}O_{SMOW}$ (6‰ to 10‰) for primary carbonatite of Taylor et al. (1967). Moreover, Yuan et al. (1995) analyzed the δD and $\delta^{18}O_{H2O}$ values of three gangue quartz samples in the deposit varying from −61‰ to −68‰ and 6.1‰ to 6.5‰, Niu et al. (1997) reported the δD and $\delta^{18}O_{H2O}$ values of five gangue quartz samples in the deposit varying from −57‰ to −72‰ and 6.2‰ to 7.75‰, we determined that the δD and $\delta^{18}O_{H2O}$ values of three gangue quartz samples in the deposit are −71‰, −74‰ and −75‰ and 7.1‰, 7.5‰ and 7.6‰, respectively. All of the H-O isotopic compositions are also within the respective ranges of the δD (−50‰ to −90‰) and $\delta^{18}O_{H2O}$ (6‰ to 10‰) for magmatic waters. Therefore, the stable isotopic compositions show that the ore-forming fluids of the Maoniuping REE deposit could be derived from a mantle source.

6 Conclusions

The Maoniuping REE deposit, Sichuan Province is the second largest primary light REE deposit in China. Fluorite is one of the main gangue minerals in the deposit, with various colors appearing in all types of ores and wallrocks. On the basis of REE geochemistry, fluorite in the deposit is classified into three types: LREE-rich, LREE-flat and LREE-depleted types. From LREE-rich to LREE-flat to LREE- depleted fluorite, the LREE%, $(La/Yb)_N$ and $(La/Sm)_N$ values tend to decrease, while the MREE%, HREE%, Sm/Nd and La/Tb values tend to increase. Y/Ho and $(Gd/Yb)_N$ do not show any obvious variation. There are good correlations between the Sm/Nd ratios and LREE%, MREE%, HREE% and Y contents. The three types of fluorite in the orefield and the Sr-Nd-Pb isotopic compositions do not show any obvious variations. These features show that the three types of fluorite in the orefield could be formed from the same sourced fluids at different stages of evolution.

The Maoniuping REE deposit is hosted in a carbonatite-syenite complex. The ore-formation age is close to those of the two types of rock. The REE contents of carbonatite and syenite in the orefield is obvious higher than those of other magmatic rocks including basalt, rhyolite and granite. The REE geochemistry of the early fluorite (LREE-rich type) is similar to those of carbonatite and syenite. Sr-Nd-Pb isotopic compositions of fluorite are close to carbonatite and syenite. C-H-O isotope show that the ore-forming fluids of the deposit could be derived from a mantle source. All these features suggest that the ore-forming fluids of the deposit are mainly derived from carbonatite and syenite melts.

Acknowledgements

This research project was financially supported jointly by the Major State Basic Research Program of People's

Republic of China (No. G1999043203), the Pre-selected Projects under the State Climbing Program (No. 95-Pre-39) and the Chinese Academy of Sciences Innovational Program (No. KZCX2-101). We thank Qi Liang in the Institute of Geochemistry, Chinese Academy of Sciences for measuring REE contents. We further thank Dr. Zhang Xingchun in the Department of Earth Science and Engineering, Imperial College, UK, and Prof. Xu Zhonglun in the Institute of Geochemistry, Chinese Academy of Sciences, whose reviews helped improve this manuscript.

Manuscript received March 30, 2006
accepted Nov. 24, 2006
edited by Liu Xinzhu

References

Alvin, M. P., Dunphy, J. M., and Groves, D. I., 2004. Nature and genesis of a carbonatite-associated fluorite deposit at Speewah, East Kimberley region, Western Australia. *Mineral. Petrol.*, 80: 127–153.

Bau, M., and Dulski, P., 1995. Comparative study of yttrium and rare–earth element behaviours in fluorine-rich hydrothermal fluids. *Contribu. Mineral. Petrol.*, 119: 213–223.

Bau, M., Romer, R. L., Lüders, V., and Dulski, P., 2003. Tracing element sources of hydrothermal mineral deposits: REE and Y distribution and Sr-Nd-Pb isotopes in fluorite from MVT deposits in the Pennine Orefield, England. *Mineralium Deposita*, 38: 992–1008.

Bill, H., and Calas, G., 1978. Color centers, associated rare-earth ions and the origin of coloration in natural fluorites. *Physics Chemistry Minerals*, 3: 117–131.

Boynton, W. V., 1984. Cosmochemistry of the rare earth elements: meteorite studies. *Dev. Geochem.*, 2: 63–114.

Bühn, B., Rankin, A.H., Schneider, J., and Dulski, P., 2002. The nature of orthomagmatic, carbonatitic fluids precipitating REE, Sr-rich fluorite: fluid-inclusion evidence from the Okorusu fluorite deposit, Namibia. *Chemical Geol.*, 186: 75–98.

Bühn, B., Schneider, J., Dulski, P., and Rankin, A.H., 2003. Fluid-rock interaction during progressive migration of carbonatitic fluids, derived from small-scale trace element and Sr, Pb isotope distribution in hydrothermal fluorite. *Geochim. Cosmochim. Acta*, 67: 4577–4595.

Bulakh, A.G., Nesterov, A.R., Zaitsev, A.N., Pilipiuk, A.N., Wall, F., and Kirillov, A.S., 2000. Sulfur-containing monazite-(Ce) from late-stage mineral assemblages at the Kandaguba and Vuoriyarvi carbonatite complexes, Kola peninsula, Russia. *Neues Jahrb. Mineral. Monatsh.*, (5): 217–233.

Chesley, J.T., Halliday, A.N., and Scrivener, R.C., 1991. Samarium-neodymium direct dating of fluorite mineralization. *Science*, 252: 949–951.

Coniglio, J., Xavier, R.P., Pinotti, L., and D'Eramo, F., 2000. Ore-Forming Fluids of Vein-Type Fluorite Deposits of the Cerro Aspero Batholith, Southern Cordoba Province, Argentina. *Inter. Geol. Rev.*, 42: 368–383.

Constantopoulos, J., 1988. Fluid inclusions and rare earth element geochemistry of fluorite from south-central Idaho. *Economic Geol.*, 83: 626–636.

Cunningham, C.G., Rasmussen, J.D., Steven, T.A., Rye, R.O., Rowley, P.D., Romberger, S.B., and Selverstone, J., 1998. Hydrothemal uranium deposits containing molybdenum and fluorite in the Marysvale volcanic field, west-central Utah. *Mineralium Deposita*, 33: 477–494.

Deans, T., and Powell, J.L., 1968. Trace elements and strontium isotopes in carbonatites, fluorites and limestones from India and Pakistan. *Nature*, 218: 750–752.

Dill, H., Dulski, P., and Möller, P., 1986. Fluorite mineralization and REE patterns in vein-type deposits from the N Bavarian Basement. *N. Jahrb. Mineral. Abh.*, 154: 141–151.

Ekambaram, V., Brookins, D.G., Rosenberg, P.E., and Emanuel, K.M., 1986. Rare-earth element geochemistry of fluorite-carbonate deposits in western Montana, USA. *Chemical Geol.*, 54: 319–331.

Eppinger, R.G., and Closs, L.G., 1990. Variation of trace elements and rare earth elements in fluorite: A possible tool for exploration. *Economic Geol.*, 85: 1896–1907.

Fanlo, I., Touray, J.C., Subias, I., and Fernandez-Nieto, C., 1998. Geochemical patterns of a sheared fluorite vein, Parzan, Spanish Central Pyrenees. *Mineralium Deposita*, 33: 620–632.

Fayziyev, A.R., 1990. Yttrium in Fluorite from Endogenous Shows in Ussr. *Geochem. Inter.*, (6): 114–119.

Gittins, J., Beckett, M.F., and Jago, B.C., 1989. Composition of the fluid phase accompanying carbonatite magma: A critical examination. *AM. Mineral.*, 75: 1106–1109.

Groves, D.I., and Vielreicher, N.M., 2001. The Phalabowra (Palabora) carbonatite-hosted magnetite- copper sulfide deposit, South Africa: an end-member of the iron-oxide copper-gold-rare earth element deposit group?. *Mineralium Deposita*, 36: 189–194.

Huang Zhilong, Xu Cheng, Liu Congqiang, Xu Deru, Li Wenbo and Guan Tao, 2003. Sr and Nd isotope geochemistry of fluorites from Maoniuping REE deposits, Sichuan Province, China: Implications for the Source of ore-forming fluids. *J. Geochem. Exploration*, 78/79: 643–648.

Jago, B.C., and Gittins, J., 1991. The role of fluorine in carbonatite magma evolutions. *Nature*, 349: 56–58.

Jiang Mingquan, 1992. The geological and structural feature of the Maoniuping REE deposit and its ore-controlling significance. *Mineral Deposits*, 11: 351–358 (in Chinese with English abstract).

McLennan, S.M., and Taylor, S.R., 1979. Rare earth element mobility associated with uranium mineralization. *Nature*, 282: 247–250.

Möller, P., Parekh, P.P., and Schneider, H.J., 1976. The application of Tb/Ca-Tb/La abundance ratios to problems of fluorite genesis. *Mineralium Deposita*, 11: 111–116.

Monecke, T., Monecke, J., Mönch, W., and Kempe, U., 2000. Mathematical analysis of rare earth element patterns of fluorites from the Ehrenfriedersdorf tin deposit, Germany: evidence for a hydrothermal mixing process of lanthanides from two different sources. *Mineral. Petrol.*, 70: 235–256.

Nasraoui, M., Toulkeridis, T., Clauer, N., and Bilal, E., 2000. Differentiated hydrothermal and meteoric alterations of the Lueshe carbonatite complex (Democratic Republic of Congo) identified by a REE study combined with a sequential acid-leaching experiment. *Chemical Geol.*, 165: 109–132.

Ngwenya, B.T., 1994. Hydrothermal rare earth mineralization in

carbonatites of the Tundulu complex, Malawi: processes at the fluid/rock interface. *Geochim. Cosmochim. Acta*, 58: 2061–2072.

Niu Hecai and Lin Chuanxian, 1994. The genesis of the Mianning REE deposits, Sichuan Province. *Mineral Deposits*, 13: 345–353 (in Chinese with English abstract).

Niu Hecai, Shan Qiang and Lin Maoqing, 1997. Fluid-melt and fluid inclusions in Mianning REE deposits, Sichuan, Southwest China. *Chinese J. Geochem.*, 16: 256–262.

Niu Hecai, Shan Qiang and Lin Maoqing, 1996. REE geochemistry of magmatogenic barite and fluorites. *Acta Mineral. Sinica*, 16: 382–388 (in Chinese with English abstract).

Pu Guangping, 1993. A discussion on metallogenetic model and prospecting targets for Maoniuping REE deposits, Sichuan Province. *Acta Geol. Sichuan*, 13: 46–57 (in Chinese with English abstract).

Qi Liang, Hu Jin, and Gregoire, D. C., 2000. Determination of trace elements in granites by inductively coupled plasma mass spectrometry. *Talanta*, 51: 507–513.

Schwinn, G., and Markl, G., 2005. REE systematics in hydrothermal fluorite. *Chemical Geol.*, 216: 225–248.

Simonetti, A., and Bell, K., 1995. Nd, Pd, and Sr isotope systematics of fluorite at the Amba Dongar carbonatite complex, India: Evidence for hydrothermal and crustal fluid mixing. *Economic Geol.*, 90: 2018–2027.

Taylor, Jr. H.P., Frechen, J., and Degens, E.T., 1967. Oxygen and carbon isotope studies of carbonatites from the Laacher See District, West Germany and the Alno District Sweden. *Geochim. Cosmochim. Acta*, 31: 407–430.

Tian Shihong, Ding Tiping, Mao Jingwen, Li Yanhe and Yuan Zhongxin, 2006. S, C, O, H isotope data and noble gas studies of the Maoniuping LREE deposit, Sichuan Province, China: A mantle connection for mineralization. *Acta Geologica Sinica* (English edition), 80: 540–549.

Wang Denghong, Yang Jianming and Yan S.H., 2001. A special orogenic type REE deposit in Maoniuping Sichuan, China: geology and geochemistry. *Resource Geol.*, 51: 177–188.

Wendlandt, R.F., and Harrison, W.J., 1979. Rare earth partitioning between immiscible carbonate and silicate liquids and CO_2 vapor: result and implications for the formation of light rare earth-enriched rocks. *Contribu. Mineral. Petrol.*, 69: 409–419.

Wood, S.A., 1990. The aqueous geochemistry of the rare-earth elements and yttrium. II. Theeoretical predictions of speciation in hydrothermal solutions to 350°C at saturation water vapor pressure. *Chemical Geol.*, 89: 99–125.

Xu Cheng, Huang Zhilong, Liu Congqiang, Qi Liang, Li Wenbo and Guan Tao, 2003. The geochemistry of carbonatites in Maoniuping REE deposit, Sichuan Province, China. *Sci. China* (D), 46: 246–256.

Xu Cheng, Zhang Huan, Huang Zhilong, Liu Congqiang, Qi Liang and Li Wenbo, 2004. Genesis of the carbonatite-syenite complex and REE deposit at maoniuping, Sichuan Province, China: Evidence from Pb isotope geochemistry. *Geochem. J.*, 38: 67–76.

Xu Jiuhua, Xie Yuling, Li Jianping and Hou Zengqian, 2001. The Sr- and LREE-bearing daughter minerals in fluid inclusions from Maoniuping REE deposits, Sichuan Province, China. *Proc. Natural Sci.*, 11: 543–547 (in Chinese with English abstract).

Yang Zhengxi, Williams-Jones, A. F., and Pu Guangping, 2001. A fluid inclusion study of Maoniuping REE deposits, Sichuan Province. *J. Mineral. Petrol.*, 21(2): 26–33 (in Chinese with English abstract).

Yang Zhengxi, Williams-Jones, A.F., and Pu Guangping, 2000. Geological features of Maoniuping REE deposits, Sichuan, China. *J. Mineral. Petrol.*, 20(2): 28–34 (in Chinese with English abstract).

Yuan Zhongxin, Bai Ge, Ding Xiaoshi, Shi Zemin and Li Xiaoyu, 1993. U-Pb isotopic age of zircon from the Maoniuping alkali granite, Sichuan Province and its geological significance. *Mineral Deposits*, 12: 189–192 (in Chinese with English abstract).

Yuan Zhongxin, Shi Zemin and Bai Ge, 1995. *The Maoniuping Rare Earth Ore Deposit, Mianning County, Sichuan Province*. Beijing: Geological Publishing House. 1–175. (in Chinese with English abstract).

Zaitsev, A.N., Demény, A., Sindern, S., and Wall, F., 2002. Burbankite group minerals and their alteration in rare earth carbonatitessource of elements and fluids (evidence from C-O and Sr-Nd isotopic data). *Lithos*, 62: 15–33.

Zartman, R.E., and Doe, B.R., 1981. Plumbotectonics-the model. *Tectonophys*, 75: 135–162.

Zhang Yunxiang, Luo Yaonan and Yang Congxi, 1988. *Panzhihua-Xichang Rift in China*. Beijing: Geological Publishing House. 1–325. (in Chinese with English abstract).

Zindler, A., and Hart, S.R., 1986. Chemical geodynamics. *Ann. Rev. Earth Planet. Sci.*, 14: 493–571.

Appendix

The REE contents of various magmatic rocks in the Maoniuping REE deposit

Name	Carbonatite								Syenite						Granite				
Sample No.	MNP-6	MNP-10	MNP-11	MNP-13	MNP-15	MNP-125	MNP-142	MNP-16-1	MNP-15	MNP-24	MNP-42	MNP-70	MNP-88	MNP-92	MNP-32	MNP-46	MNP-50	MNP-59	MNP-61
La	454	648	524	828	786	475	794	514	198	945	385	215	136	127	36.6	45.6	63.3	61.9	38.1
Ce	916	1395	1143	1628	1708	1043	1730	1079	310	1604	513	245	215	119	65.9	102	147	140	76.5
Pr	94.7	142	120	160	159	111	176	110	30.1	153	46.2	27.5	20.2	15.9	7.13	10.7	14.6	14.6	7.85
Nd	377	542	468	599	686	427	687	422	93.4	481	132	86.6	64.5	49.1	23.4	38.9	51.3	51.7	25.9
Sm	65.1	74.7	74.3	84.4	98.4	69.9	99.5	63.5	12.9	52.7	12.1	9.78	8.86	7.36	4.71	7.93	11.5	11.0	5.18
Eu	15.0	16.4	16.4	18.4	21.0	15.7	20.8	14.4	2.93	11.1	2.02	2.53	2.25	1.81	0.54	0.62	0.64	0.56	0.65
Gd	49.1	50.3	53.0	59.2	65.4	49.5	65.6	45.5	6.54	29.3	7.80	6.17	5.21	5.68	4.34	7.79	11.03	9.98	5.09
Tb	6.18	5.53	6.27	6.62	7.22	5.83	7.33	5.2	0.74	3.23	0.98	0.69	0.65	0.92	0.73	1.55	2.33	1.66	0.93
Dy	31.0	25.3	29.7	30.7	32.8	27.7	33.2	24.4	2.83	12.9	5.30	2.97	3.04	5.13	4.48	9.10	14.76	9.87	5.56
Ho	5.68	4.16	5.04	5.1	5.27	4.62	5.46	4.33	0.44	1.96	1.05	0.53	0.49	1.01	0.93	1.97	3.10	1.99	1.17
Er	17.3	12.7	15.1	15.8	16.1	13.9	16.2	13.1	1.06	4.59	3.08	1.23	1.22	2.83	2.78	5.48	9.27	5.81	3.51
Tm	2.38	1.53	1.94	1.97	1.96	1.78	2.00	1.65	0.14	0.55	0.48	0.15	0.17	0.47	0.45	0.87	1.48	1.02	0.55
Yb	15.7	10.1	12.0	12.6	12.6	11.4	12.7	10.8	0.94	2.98	3.58	1.02	1.22	3.23	3.30	6.06	10.36	6.96	4.08
Lu	2.03	1.24	1.53	1.57	1.45	1.40	1.55	1.33	0.11	0.31	0.53	0.13	0.17	0.50	0.51	0.83	1.39	0.99	0.57
Y	156	131	149	151	152	139	157	133	15.8	52.2	31.4	16.4	17.7	29.3	28.8	56.0	89.4	60.2	35.8
ΣREE	2051	2929	2470	3451	3601	2258	3651	2309	660	3303	1113	599	459	340	156	240	342	318	176
Data source	Xu et al. (2003)								Xu et al. (2003)						This paper				

(Continued)

Name	Granite													Rhyolite			Basalt		
Sample No.	MNP-73	MNP-25	MNP-27	MNP-44	MNP-54	MNP-56	MNP-60	MNP-65	MNP-30	MNP-31	MNP-39	MNP-51	MNP-71	MNP-78	MNP-89	MNP-135	MNP-35	MNP-40	MNP-45
La	46.0	43.2	40.6	38.1	65.6	43.7	46.1	95.4	56.8	23.9	33.8	50.5	53.9	35.6	16.9	48.8	20.7	20.6	38.0
Ce	78.4	83.4	81.3	76.4	114	87.1	88.6	159	118	45.7	44.9	110	84.4	59.0	42.6	66.2	43.7	41.4	78.1
Pr	8.91	8.74	8.19	7.93	11.6	8.87	9.13	17.4	13.2	4.62	6.28	10.3	9.96	6.72	3.03	8.41	5.95	4.77	8.90
Nd	30.4	29.8	27.6	26.0	38.0	30.4	31.3	57.4	46.6	15.1	21.9	34.7	32.5	22.4	8.95	27.6	25.6	17.8	33.3
Sm	6.42	5.81	5.33	5.31	7.44	6.10	5.77	9.54	9.86	3.35	4.63	7.39	6.23	4.64	2.15	4.82	6.80	3.92	6.56
Eu	0.73	0.63	0.62	0.66	1.03	0.69	0.77	1.24	0.55	0.28	0.59	0.40	0.69	0.80	0.24	0.70	2.16	1.23	1.56
Gd	6.00	5.43	4.93	4.90	7.11	5.67	5.40	8.17	9.95	3.38	4.63	7.55	5.87	3.99	2.41	4.14	7.49	4.20	5.66
Tb	0.98	0.96	0.92	0.87	1.23	1.02	0.93	1.30	1.82	0.64	0.79	1.48	1.03	0.68	0.52	0.66	1.23	0.72	0.96
Dy	6.12	5.81	5.67	5.36	8.40	6.12	5.49	7.71	11.60	3.77	4.97	9.66	5.90	4.50	3.64	3.96	7.47	4.13	5.05
Ho	1.23	1.21	1.13	1.08	1.83	1.24	1.16	1.61	2.47	0.76	1.01	2.10	1.16	0.94	0.82	0.88	1.46	0.89	1.11
Er	3.50	3.37	3.20	3.26	5.43	3.69	3.43	4.89	7.13	2.24	2.94	6.16	3.42	2.54	2.44	2.62	3.88	2.47	3.02
Tm	0.61	0.53	0.50	0.55	0.86	0.59	0.58	0.75	1.16	0.36	0.45	1.07	0.60	0.38	0.43	0.47	0.56	0.39	0.45
Yb	4.05	3.96	3.49	3.66	6.55	3.89	4.12	5.80	7.72	2.74	3.28	7.67	4.51	2.72	3.26	3.57	3.77	2.63	3.18
Lu	0.56	0.55	0.51	0.55	0.91	0.56	0.62	0.87	1.12	0.43	0.46	1.05	0.59	0.43	0.47	0.54	0.54	0.36	0.45
Y	37.3	36.3	34.7	33.7	60.9	38.2	36.6	53.0	72.8	24.2	30.7	64.4	35.7	25.2	24.1	26.5	39.6	25.3	30.0
ΣREE	194	193	184	175	270	200	203	371	288	107	131	250	211	145	87.9	173	131	105	186
Data source	This paper													This paper			This paper		